Knockout of zebrafish desmin genes does not cause skeletal muscle degeneration but alters calcium flux.

Gulsum Kayman Kurekci[1], Ecem Kural Mangit[1,2], Cansu Koyunlar[1,3], Seyda Unsal[1], Berk Saglam[4], Bora Ergin[4], Ismail Uyanik[5], Niloufar Boustanabadimaralan Düz[1], Beril Talim[6], Nuhan Purali[4], Simon M. Hughes[7], Pervin R. Dincer[1]*.

[1]Department of Medical Biology, Hacettepe University Faculty of Medicine, Ankara, 06100, Turkey.

[2]Laboratory Animals Research and Application Centre, Hacettepe University, Ankara, 06100, Turkey

[3]Current address: Department of Hematology, Erasmus MC, Rotterdam, 3015 CN, The Netherlands

[4]Department of Biophysics, Hacettepe University Faculty of Medicine, Ankara, 06100, Turkey.

[5]Department of Electrical and Electronics Engineering, Hacettepe University Faculty of Engineering, Ankara, 06800, Turkey.

[6]Department of Pediatrics, Pathology Unit, Hacettepe University Faculty of Medicine, Ankara, 06100, Turkey.

[7]Randall Centre for Cell and Molecular Biophysics, New Hunt's House, Guy's Campus, King's College London, London, SE1 1UL, United Kingdom.

*Corresponding author.

Abstract

Desmin is a muscle-specific intermediate filament protein that has fundamental role in muscle structure and force transmission. Whereas human desmin protein is encoded by a single gene, two desmin paralogs (*desma* and *desmb*) exist in zebrafish. *Desma* and *desmb* show differential spatiotemporal expression during zebrafish embryonic and larval development, being similarly expressed in skeletal muscle until hatching, after which expression of *desmb* shifts to gut smooth muscle. We generated knockout (KO) mutant lines carrying loss-of-function mutations for each gene by using CRISPR/Cas9. *Desma*;*desmb* double mutants are viable and fertile, and lack obvious skeletal muscle, heart or intestinal defects. In contrast to morphants, knockout of each gene did

not cause any overt muscular phenotype, but did alter calcium flux in myofibres. These results point to a possible compensation mechanism in these mutant lines generated by targeting nonsense mutations to the first coding exon.

Introduction

Desmin is a type III intermediate filament protein that is specifically expressed in skeletal, cardiac and smooth muscles. In addition to their fundamental role in maintaining the structural integrity of the sarcomere, desmin intermediate filaments are involved in mechanotransduction and organelle positioning. Desminopathies belonging to myofibrillar myopathies are primarily characterized by abnormal protein aggregates in muscle and present as progressive skeletal myopathy and/or cardiomyopathy[1]. Although the involvement of smooth muscles is not widely reported, some patients suffer from smooth muscle dysfunction such as swallowing difficulties, intestinal pseudo-obstruction and respiratory insufficiency[2–4]. The majority of desmin mutations are associated with desmin aggregates; however, some mutations have been reported to not alter filament assembly and network integrity *in vivo* or *in vitro*[5,6]. KO of desmin in mice does not affect the viability and the development of muscles; however, muscle degeneration and cardiomyopathy are observed[7,8].

Zebrafish is a widely used model for neuromuscular disorders[9,10]. Besides the advantage of being the most abundant tissue in zebrafish; the gene profile, and the structural and histological features of mammalian skeletal muscle are highly preserved in zebrafish[11]. To date, two approaches have been used to study the effect of the loss of desmin in zebrafish. On one hand, it was shown that morpholino-mediated knockdown of desmin causes skeletal and cardiac muscle myopathy[12,13]. On the other hand, Ramspacher et al. studied a desmin mutant line (*desma*^{sa5}), generated by ENU mutagenesis, which causes a truncation mutation approximately half way along the molecule, that also presented with skeletal and cardiac muscle phenotype[14].

Gene duplications are common in zebrafish and most duplicated genes have similar functions to their human orthologs. Alternatively, paralogs can be expressed in different tissues or stages of development and have distinct functions to their human orthologs. Humans carry a single copy of the *DES* gene whereas two desmin genes (*desma* and *desmb*) are found in zebrafish[13]. Previous work has not established the tissue specific distribution and role of these two desmin paralogs.

Here, we report the spatiotemporal expression pattern of the two desmin paralogs in zebrafish, as well as the generation using CRISPR/Cas9 and characterization of putative null zebrafish mutant lines for each of the desmin paralogs. We show that *desma* and *desmb* are expressed in skeletal muscle until 72-hour post-fertilization (hpf). After 72 hpf, expression of *desmb* shifts to gut smooth muscle. Putative null mutation of each gene does not affect viability and adults do not develop any overt phenotype. However, altered calcium flux was observed in *desma*-KO myofibres. Surprisingly, *desma;desmb* double mutants also survive to adulthood with no sign of muscle defect. These results show that loss-of-function of desmin genes by mutations in the first coding exon result in a mild phenotype with no visible muscle degeneration but altered calcium flux, in contrast to morpholino-mediated knockdown models and the $desma^{sa5}$ allele.

RESULTS

Zebrafish desmin genes

Zebrafish have two *desmin* orthologs, *desma* (*desmin a*) and *desmb (desmin b)*, which are located on chromosome 9 and 6, respectively. *Desma* and *desmb* paralogs share 81% and 83% identity with human *DES* gene. Although a single transcript is known to be encoded by human *DES* gene, in ENSEMBL two isoforms are predicted to be transcribed from *desma*, *desma-1* mRNA coding for a 488 amino acid protein (predicted molecular weight of 55.7 kDa) and *desma-2* mRNA coding for a 473 amino acid protein (predicted molecular weight of 54.1 kDa). In *desma-2* transcript, exon 9 is skipped, corresponding to 15 amino acid located in the tail domain of Desma-1 protein (Supplementary Fig. S1). The 473 amino acid Desmb protein is predicted to have a molecular weight of 54.2 kDa. At the amino acid level, Desma-1, Desma-2 and Desmb show 80%, 82% and 83% similarity with human desmin protein.

Differential expression of desmin transcripts during zebrafish development

We analyzed the spatiotemporal expression patterns of *desma* and *desmb* genes during zebrafish development at several stages beginning from somitogenesis until 5 days post fertilization (dpf) by whole mount *in situ* hybridization (ISH). For detecting both *desma* transcripts (*desma-2* lacks exon 9), we synthesized an antisense probe by using a forward primer binding to exon 1 and a reverse primer binding to exon 10 (Supplementary Fig. S1). No specific staining was observed in embryos treated with sense probes for each gene (Supplementary Fig. S2). *Desma* was first

88 detected at 11 hpf in adaxial slow muscle precursor cells when the first somites form and remained
89 strongly expressed in somites at all examined stages (Fig. 1a). *Desma* was also expressed in the
90 developing heart from 35 hpf (Fig. 1b). Cryosections of 72 hpf embryos showed that *desma* was
91 distributed in the entire somite, including epaxial and hypaxial muscles (Fig. 1c). By 72 hpf, *desma*
92 was expressed in cranial muscles including external ocular muscles, opercular muscles and
93 mandibular muscles (Fig. 1d). At 96 hpf, transversal sections revealed *desma* expression at the
94 anterior intestine (Fig. 1d, upper panel). At 72, 96 and 120 hpf, expression of *desma* in pectoral
95 fin muscles was clearly visible (Fig. 1d). *Desmb* had an overlapping expression pattern to *desma*
96 from the beginning of somitogenesis until 72 hpf, including staining in trunk somites and heart
97 (Fig. 1a, b). At 72 hpf, somitic expression of *desmb* dramatically decreased with a residual
98 expression in the lateral edges of the myotome. By contrast, strong signal of *desmb* transcripts was
99 detected around the gut throughout the length of the intestine (Fig. 1a, c, e). Similar to *desma*,
100 *desmb* was also expressed in pectoral fin muscles, operculum muscles and mandibular muscles at
101 72 hpf (Fig. 1e). These results indicate that *desma* and *desmb* expression partially overlap during
102 zebrafish muscle development. As the gut develops, *desmb* expression shifts from somitic muscle
103 to gut smooth muscle.

104 **Generation of *desma* and *desmb* knockout zebrafish lines**

105 *Desma* and *desmb* mutant zebrafish lines were generated by using CRISPR/Cas9 genome editing.
106 The $desma^{kg97}$ line exhibited 2 bp deletion and 4 bp insertion in the first exon
107 (g.198_99delGAinsTGAT, NC_007120.7) leading to a frameshift at amino acid 45 and a
108 premature stop codon after four amino acids. In the $desmb^{kg156}$ mutant line, a 5 bp deletion in exon
109 1 (c.245_249delCTTAT, NM_001077452.1) resulted in a frameshift at amino acid 82 and
110 introduced a premature stop codon after three amino acids (Fig. 2a). Heterozygous mutants showed
111 no defect and homozygous mutant embryos and larvae developed relatively normally, at least for
112 the first few days (Fig. 2b-f).

113 **Expression of *desma* and *desmb* in knockout lines**

114 Mutations were predicted to trigger nonsense-mediated decay of mRNA or synthesis of short
115 truncated polypeptides. As expected, qRT-PCR revealed a significant decrease of *desma*
116 transcripts in $desma^{kg97}$ homozygous embryos (P=0.0119, Mann-Whitney U), while *desmb*

117 transcripts were significantly decreased in *desmb*^{kg156} homozygous embryos at 96 hpf compared to
118 wild type (WT) (P=0.0079, Mann-Whitney U) (Fig. 2b). Consistent with El-Brolosy et al.[15], weak
119 *desmb* or *desma* mRNA up-regulation may occur in the respective mutant embryos (Fig. 2b).
120 In order to investigate the potential compensatory effect of *desmin* paralog upregulation in
121 mutant embryos, expression patterns of *desmb* and *desma* transcripts were determined in *desma*^{kg97}
122 or *desmb*^{kg156} homozygous mutant embryos, respectively. In *desma*$^{kg97/kg97}$ embryos, the expression
123 pattern of *desmb* transcripts (Fig. 2c) was similar to that of wild-type embryos (Fig. 1a). Somitic
124 expression of *desmb* was observed in *desma*$^{kg97/kg97}$ at 48 hpf, and a shift towards gut expression
125 after 72 hpf. Beyond 72 hpf, no *desmb* staining was detected in somites of *desma*$^{kg97/kg97}$ embryos.
126 In *desmb*$^{kg156/kg156}$ embryos, *desma* was still strongly expressed in somites and visible in the
127 anterior intestine at 96 hpf (Fig. 2c). In order to confirm the loss-of-function of desmin in mutants
128 at the protein level, expression of Desma and Desmb in WT, *desma*^{kg97} or *desmb*^{kg156} homozygous
129 embryos at 96 hpf was determined by immunofluorescent staining using a desmin antibody
130 recognizing both proteins (Fig. 2d-f). In WT embryos, desmin staining was detected in both
131 somites and gut (Fig. 2d). As expected from ISH results, somitic expression was lost and gut was
132 preferentially stained in *desma*$^{kg97/kg97}$ mutants (Fig. 2f). In *desmb*$^{kg156/kg156}$ mutants, expression in
133 somites and anterior intestine were preserved while staining of the middle and posterior intestine
134 was lost (Fig. 2e). We conclude that mutation of each gene reduces the cognate mRNA and protein
135 at all stages examined and that compensation by up-regulation of the unmutated paralogous gene
136 is at best very weak.

137 **General larval characteristics of desmin mutants**

138 In order to evaluate the effects of the absence of *desma* or *desmb* on development, WT, *desma*^{kg97}
139 and *desmb*^{kg156} homozygous embryos/larvae were compared. No significant difference was
140 observed in the number of viable eggs between *desma*$^{kg97/kg97}$ and WT (P=0.6842, Mann-Whitney
141 U) or *desmb*$^{kg156/kg156}$ and WT (P=0.9654, Mann-Whitney U) (Fig. 3a). Hatching period (48-72
142 hpf[16]) is a critical process in embryonic development and reduction in the hatching rate could be
143 associated with reduced muscle function[17]. The time course showed that although different
144 hatching times were observed between groups, no significant difference was found between
145 hatching rates of mutant and WT embryos at 72 hpf with over 94% of embryos hatched

146 (*desma*$^{kg97/kg97}$ vs. WT, *P*=0.9902; *desmb*$^{kg156/kg156}$ vs WT, *P*=0.3186, repeated measures two-way
147 ANOVA, Bonferroni post *hoc* test) (Fig. 3b).
148 Similar mortality rates were observed with no significant difference between homozygous
149 mutants of *desma*^{kg97} or *desmb*^{kg156} and WT embryos (*desma*$^{kg97/kg97}$ vs. WT, *P*=0.1287;
150 *desmb*$^{kg156/kg156}$ vs. WT, *P*=0.6239, repeated measures two-way ANOVA) (Fig. 3d). Finally,
151 among surviving larvae, no statistically significant difference in body length was observed
152 between WT and mutant groups (*P*=0.2036 for WT vs. *desma*$^{kg97/kg97}$; *P*=0.1893 for WT vs.
153 *desmb*$^{kg156/kg156}$, Mann-Whitney U) (Fig. 3c).

154 **Mutant larvae show no neuromuscular defect**

155 Muscle fibre integrity and somite morphology length were investigated by staining muscle actin
156 with rhodamine phalloidin in 96 hpf embryos (Fig. 3e). At this stage, mainly *desma* is expressed
157 in somites. No muscle lesion or detachment of fibres was observed in mutants and no significant
158 difference was found in somitic length between mutants and WT (*P*=0.7912 for WT vs.
159 *desma*$^{kg97/kg97}$; *P*=0.4923 for WT vs. *desmb*$^{kg156/kg156}$, Mann-Whitney U) (Fig. 3f).
160 Touch-evoked response assay is a widely used method to assess neuromuscular function
161 in 48 hpf zebrafish embryos[18]. We performed motility experiments in a blinded manner on siblings
162 from three groups of heterozygous mutant in-crosses and genotyped them after. First, the average
163 escape time of siblings from *desma*$^{kg97/+}$ in-crosses was assessed and no significant difference was
164 found in *desma*^{kg97} heterozygous (*P*=0.122, Mann-Whitney U) or homozygous (*P*=0.5529, Mann-
165 Whitney U) mutants compared to WT (Fig. 3g). Similarly, no significant difference in the average
166 escape time was found in *desmb*^{kg156} heterozygous (*P*=0.3968, Mann-Whitney U) or homozygous
167 (*P*=0.6131, Mann-Whitney U) mutants compared to WT (Fig. 3h). Since both *desma* and *desmb*
168 are expressed in somites up to this stage (48 hpf) and might potentially compensate for the absence
169 of each other, we finally evaluated the effect of the absence of both proteins in siblings from
170 *desma*$^{kg97/+}$;*desmb*$^{kg156/kg156}$ double mutants. No significant difference in the average escape time
171 was found in homozygous double mutants (*desma*$^{kg97/kg97}$;*desmb*$^{kg156/kg156}$) compared to
172 *desma*$^{+/+}$;*desmb*$^{kg156/kg156}$ (*P*=0.3165, Mann-Whitney U) and in *desma*$^{kg97/+}$;*desmb*$^{kg156/kg156}$
173 embryos compared to *desma*$^{+/+}$;*desmb*$^{kg156/kg156}$ (*P* = 0.2334, Mann-Whitney U) (Fig. 3i).

174 **Mutant adult skeletal muscle shows no muscle degeneration**

175 Because no skeletal muscle phenotype was observed in mutant larvae, surviving one-year-old
176 adults were investigated for muscle defects. Some homozygous single and double mutants
177 survived until adulthood with no sign of behavioral defect. Western blot was performed using
178 myotomal skeletal muscle protein extracts isolated from adult fish (WT, homozgous and
179 heterozygous *desma*^{kg97} mutants, homozygous and heterozygous *desmb*^{kg156} mutants and
180 *desma*$^{kg97/kg97}$;*desmb*$^{kg156/kg156}$ double mutants). As *desma* was shown to be predominantly
181 expressed in somites from 72 to 120 hpf, the two bands detected in WT and *desmb*^{kg156} mutants
182 were predicted to correspond to Desma-1 (predicted molecular weight 55.7 kDa) and Desma-2
183 (predicted molecular weight 54.1 kDa) isoforms. In agreement with that, both bands were absent
184 in *desma*^{kg97} homozygous mutant and double mutants while still expressed in homozygous
185 *desmb*^{kg156} mutant (Fig. 4a). Nevertheless, histopathological examination of hematoxylin-eosin
186 stained skeletal muscle tissue sections revealed no pathological changes in homozygous single or
187 double mutants (Fig. 4b). General morphology of skeletal fibre shape and size, integrity of
188 sarcoplasm was normal. There was an absence of cytoplasmic aggregates, signs of degeneration
189 or regeneration, internal nuclei, inflammatory cell infiltration, increase in connective or adipose
190 tissue in interstitium (Fig. 4b). We conclude that fish entirely lacking wild-type desmin generate
191 and maintain functional skeletal muscle in the context of a zebrafish aquarium.

192 **Altered calcium flux in *desma* mutant fibres**

193 Although anatomically apparently wild-type, adult *desma*$^{kg97/kg97}$ mutants were physiologically
194 defective in calcium handling. To investigate amplitude and time course of calcium signals
195 released in response to a depolarizing voltage stimulus, individual fibres were dissected from WT
196 (N=8), *desma*^{kg97} (N=11) or *desmb*^{kg156} (N=8) homozygous mutant 1-year-old fish. Calcium flux
197 along fibres was monitored in the isolated fibres by Fluo-4 AM after four consecutive depolarizing
198 stimuli with the amplitude of the current pulse kept constant at 100 nA and the duration increased
199 by 10 ms at each pulse (Fig. 5a-b). Amplitudes of the calcium emission signals in the first (10 ms)
200 stimulus and fourth (40 ms) stimulus were compared between mutants and WT. To eliminate
201 variance induced by amplitude, offset and fibre size differences, amplitude values were baseline
202 corrected and divided by the diameter of each fibre. Amplitudes of the first or the fourth calcium
203 transient were significantly lower in *desma*$^{kg97/kg97}$ fibres compared to WT fibres (P=0.0008 for

204 first transient; P=0.0025 for fourth transient, Mann-Whitney U) (Fig. 5c-d). In contrast, no
205 significant difference was found in the amplitude of calcium flux between *desmb*$^{kg156/kg156}$ fibres
206 and WT fibres (P=0.0881 for first transient; P=0.6657 for fourth transient, Mann-Whitney U) (Fig.
207 5c-d).

208 Time course of the longest calcium transient (40 ms, fourth transient) has been analyzed
209 for comparing the waveform of the responses and dissecting each phase of the transient. Signals
210 have been baseline corrected and then normalized. Mean amplitude values as a function of time
211 were compared between *desma*$^{kg97/kg97}$ and WT or *desmb*$^{kg156/kg156}$ and WT. No significant
212 difference was found in the rising and the plateau phases of the recorded transients between the
213 experimental groups (Figure 5e). However, the decay phase was significantly faster in
214 *desma*$^{kg97/kg97}$ mutant fibres compared to WT (* indicates P<0.05, repeated measures ANOVA,
215 Bonferroni post *hoc* test). No significant difference was found in *desmb*$^{kg156/kg156}$ mutant fibres
216 compared to WT (Fig. 5e).

217 DISCUSSION

218 We demonstrated differential expression of *desma* and *desmb* paralogs during zebrafish
219 development. Although previous studies showed that *desma* is the main gene expressed in somites,
220 no study did clearly distinguish the spatial and temporal differences in the expression of the two
221 genes. We showed that until 72 hpf *desma* and *desmb* expression overlap but later in development,
222 their expression diverges. While *desmb* expression shifts from somites to gut, *desma* remains as
223 the predominantly expressed paralog in somites. Note that the residual *desmb* expression detected
224 in the lateral edges of the myotome might reflect a transient expression in new muscle fibres[19].
225 Reduction of Desmin protein in adult *desma* mutants confirms that Desma is the major desmin
226 protein in adult zebrafish skeletal muscle. Desmb appears the major desmin in smooth muscle, at
227 least in the gut. So zebrafish *desmb* mutants may be particularly useful for understanding the role
228 of desmin in smooth muscle without interference by additional phenotypes from skeletal muscle.
229 In future studies, it will be necessary to take into account this divergent expression when studying
230 the role of desmin in zebrafish.

231 Reduced *desma* or *desmb* mRNAs in their respective mutants suggest the mRNAs are
232 degraded by nonsense-mediated decay, such that only tiny amounts of the severely truncated
233 proteins would be produced. Such fragments lack the highly conserved α-helical central rod

234 domain responsible for filament formation and all known protein-protein interaction domains of
235 Desmin[20]. Intriguingly, no overt phenotype was observed in some double homozygous mutants.
236 In contrast to desmin morphants where both *desma* and *desmb* were targeted with morpholinos [13],
237 we found that *desma*^{kg97} or *desmb*^{kg156} alleles have no effect on hatching of eggs, mortality rate and
238 length of larvae. While motility is altered in 48 hpf desmin morphants, no significant alteration
239 was detected in *desma*^{sa5} embryos[13,21]. By reasoning that this could be due to a compensation by
240 *desmb*, which is still expressed in somites at 48 hpf, we performed motility assays in both single
241 mutant and double mutant embryos but found no additional neuromuscular defect in larvae mutant
242 in single or both desmin genes. At the histological level, no sign of muscle degeneration or
243 disorganisation of fibres was observed in *desma*^{kg97} or *desm*b^{kg156} mutant skeletal muscles in either
244 embryos and adults. In contrast, the desmin morphants and *desma*^{sa5} mutant muscles of embryos
245 were disorganized, with disruption of sarcomeres[13,14]. Our findings raise the possibility that a
246 haploinsufficient dominant effect in *desma*^{sa5} mutants may disrupt muscle; such an explanation
247 would no account for the morphant phenotype. We conclude that at least two further alleles of
248 *desma* may be needed to resolve these differences: firstly, a deletion allele that would
249 simultaneously prevent any Desma polypeptide synthesis and any RNA-triggered compensation
250 and, secondly, an allele lacking morpholino binding ability but nevertheless encoding wild-type
251 protein to prove that the morphant phenotype is due to *desma* binding.

252 We found that the amplitude of calcium signals released in response to a depolarizing
253 current stimulus applied to fibres was significantly lower in *desma*^{kg97} compared to WT. In
254 addition, while rising and plateau phases of calcium signals were similar between all groups, the
255 decay phase was shorter in *desma*^{kg97} mutants compared to WT. These results indicate that
256 mechanisms regulating cytosolic calcium are altered and fibres are not efficient in generating a
257 long lasting calcium increase in the absence of desmin. These results are concordant with calcium
258 flux defects observed in desmin mutant mice and hearts of *desma*^{sa5} embryos[14]. Our data support
259 the idea that desmin has a similar role in calcium conduction in skeletal muscle fibres and suggest
260 that some aspects of the *desma*^{sa5} phenotype may reflect loss of function of Desma.

261 Although not the focus of this study, it should be noted that heart and gastroinstestinal
262 development in mutant lines have not been extensively analyzed. No heart oedema such as
263 observed in desmin morphant or overt morphological abnormality in the gut have been observed
264 in *desma*^{kg97}, *desmb*^{kg156} or double mutant embryos and adults.

265 Many loss-of-function mutants not exhibiting an overt phenotype and failing to phenocopy
266 morphants have been previously reported[22–24]. El-Brolosy et al. proposed transcriptional
267 adaptation triggered by mutant RNA degradation as a mechanism to explain this discrepancy[15,25].
268 According to this model, decay of the mutant mRNA results in upregulation of related genes,
269 alleviating or suppressing the phenotype observed in morphants. Such adaptation could explain
270 the milder phenotype observed in mutants created in our study compared to desmin morphants.
271 However, it has been shown that *desma*^{sa5} allele results in a muscle phenotype similar to that of
272 morphants, even though the *desma*^{sa5} allele predicts an in-frame stop codon and no *desma* mRNA
273 was detected in mutants[14,21]. We also observe a severe reduction in *desma* mRNA in our *desma*^{kg97}
274 mutant. The specific mechanism leading to the absence of mRNA was not investigated either in
275 *desma*^{sa5} mutants or in the present study. It is possible that the *desma*^{sa5} allele is not as efficient as
276 *desma*^{kg97} allele in triggering an adaptation mechanism for yet unknown reasons. However, our
277 data suggest that the compensating gene in fish carrying our *desma* allele is not *desmb*, the only
278 gene known to have high and extensive homology to *desma*. It will be interesting to compare these
279 models in the contexts of mRNA decay and transcriptional adaptation. Alternatively, short
280 truncated polypeptides not detected in Western blot might play a role in this process before being
281 rapidly degraded. In conclusion, unraveling modifier genes and proteins that compensate for the
282 loss of desmin in our models will bring further insights in the role of desmin in muscle.

283 # METHODS

284 **Ethical approval and zebrafish maintenance**

285 All animal procedures were performed in accordance with Turkish *Animal Protection Act* 2004
286 and later modifications conforming to all relevant guidelines and regulations, and approved by the
287 Hacettepe University Animal Experimentations Local Ethics Board (Approval no. 2014/07-08).
288 The work in the UK was performed under UK Home Office licence in accordance with the UK
289 Animal (Scientific Procedures) Act 1986 and subsequent modifications. Adult zebrafish (AB)
290 (*Danio rerio*) were kept in 14/10 hr light-dark cycle at 28.5ºC. Adults are fed twice a day, with
291 dry feed in morning and *Artemia spp.* in evening. For spawning, male and female fish were placed
292 in a breeding tank with a separator. Next morning the separator was removed, viable eggs were
293 collected and rinsed in E3 medium (5 mM NaCl, 0.17 mM KCl, 0.33 mM $CaCl_2$, 0.33 mM $MgSO_4$,

294 10^{-5}% Methylene Blue). Embryos were kept in E3 medium for five days and placed into adult
295 tanks containing system water. Embryos were fed five times a day with dry feed and Artemia.

296 **Whole mount *in situ* hybridization**

297 Embryos were fixed in 4% PFA in PBS (w/v) overnight at 4°C, dehydrated in 50% and %100
298 methanol washes and stored at -20°C at least overnight before use. Probe templates were amplified
299 from cDNA isolated from 96 hpf wild-type embryos. Reverse primers for antisense probe
300 contained T3 promoter sequence while forward primers for sense probes contained T7 promoter
301 sequence. Primers sequences can be found as Supplementary Table S1 online. Digoxigenin-
302 labelled probes were generated using T3 or T7 RNA polymerases. Whole mount *in situ* mRNA
303 hybridization was performed as described[26]. Embryos were photographed as on Zeiss Axiophot
304 with Axiocam (Carl Zeiss, Oberkochen, Germany) using Openlab software (Agilent, Santa Clara,
305 CA, USA).

306 **Generation of mutant zebrafish lines**

307 CRISPR-Cas9 genome editing was performed as described in Fin et al[24]. CRISPR-Cas9 sgRNAs
308 showing minimal off-target sites were designed by using the online software ZiFiT Targeter.
309 Oligos encoding sgRNAs targeting the first exon of *desma* (GRCz11, Chr9: 7539113-7539132,
310 GGTCACCTCGTAAACTCTGG) and *desmb* (GRCz11, Chr6: 13891417-13891437,
311 GGCTATACTCGCTCTTATGG) were cloned into pDR274 plasmid (Addgene). sgRNAs were
312 synthesized using T7 RiboMAX Large Scale RNA production system (Promega) following the
313 manufacturer's protocol. Transcribed sgRNAs were purified using sodium acetate and ethanol
314 precipitation and quantified on Qubit fluorometer. Cas9 mRNA was transcribed from pCS2-Cas9
315 plasmid using mMessage mMachine SP6 Kit (Ambion) and purified by lithium chloride
316 precipitation. One-cell stage embryos were injected with 2 nl containing 80-200 pg of sgRNA and
317 100 pg of Cas9 mRNA. At 48 hpf, ten embryos were analysed for mosaicism at targeted loci using
318 high resolution melt analysis. Injected embryos were raised to adulthood and back-crossed to
319 identify transmitted mutations in F1 progeny. Homozygotes for each gene were generated by in-
320 cross of F2 heterozygotes. Primers sequences used for genotyping by Sanger sequencing can be
321 found as Supplementary Table S1 online.

322 **Quantitative real-time PCR**

323 Total RNA was isolated from a pool of 20 mechanically homogenized embryos at 96 hpf for each
324 sample (n=8) using TRItidy G (AppliChem) and 500 ng of cDNA was synthesized using
325 QuantiTect Reverse Transcription Kit (Qiagen) according to manufacturer's protocol. Primer
326 sequences for *desma* (covering both *desma-1* and *desma-2*), *desmb* and *actb1* can be found as
327 Supplementary Table S1 online. qPCR was performed in triplicates using SensiFAST SYBR No-
328 ROX Kit (Bioline) in Rotor-Gene 6000 (Corbett Life Science). *Desma* and *desmb* expression
329 levels were normalized to *actb1* expression, mutant expression levels were calculated relative to
330 wild-type using ΔΔCt method[27].

331 **Protein Extraction and Immunoblotting**

332 For protein extraction, 1-year-old fish were euthanized using overdose of tricaine (MS222, 300
333 mg/l). Skeletal muscle tissue was immediately dissected and fresh-frozen in liquid nitrogen. Tissue
334 was pulverized and homogenized in blending buffer (16 M Tris HCl, 200 M EDTA, 20% SDS,
335 1X protease inhibitor cocktail, volume adjusted to 5 ml with dH_2O) by sonication on ice. Lysates
336 were then centrifuged and supernatant transferred in a fresh tube. Total protein concentrations were
337 determined by bicinchoninic acid Protein Assay (Pierce, 23225). Equal amounts of protein (40 µg)
338 were loaded on a 13% polyacrylamide gel and transferred onto a nitrocellulose membrane using
339 semi-dry transfer, blocked for one hour at room temperature (%5 nonfat dried milk in %0,2 TBS-
340 T) and probed with anti-desmin antibody (1:1000; Sigma, D8281) overnight at 4°C or anti-lamin
341 B1 antibody (Abcam, ab90169) followed by appropriate HRP-conjugated secondary antibody.
342 Chemiluminescence detection was done by using SuperSignal™ West Femto Maximum Sensivity
343 substrate (Thermo Scientific, 34095) in GeneGnome device.

344 **Whole-mount Immunofluorescence**

345 96 hpf embryos were fixed in %4 PFA overnight at +4°C and washed with PBTx (%0.01 Triton
346 X-100 in PBS). Embryos were permeabilized in 50 µg/ml Proteinase K for 2 hours and re-fixed in
347 2% PFA for 20 minutes at room temperature. Embryos were blocked in %5 BSA for 2 h at room
348 temperature and incubated with anti-desmin antibody (1:20; Sigma, D8281) for two overnights.
349 After two overnight incubations with Alexa-Fluor 488 conjugated secondary antibody, embryos
350 were mounted with DAPI onto glass bottom dishes for imaging with Zeiss LSM Pascal laser
351 scanning confocal microscope.

352 **Larval Phenotype and Morphology**

353 After successful mating, embryos were collected, counted and recorded for the following rates.
354 Hatching rate was reported as cumulative percentage of hatched embryos at 24 hpf, 48 hpf and 72
355 hpf. Mortality rate was expressed as the percentage of death embryos for 5 dpf. For body length
356 measurements, at least 16 embryos at 96 hpf were mounted, photographed (The Imaging Source,
357 DFK 41AU02) and measured from the mouth tip to the tail base using ImageJ (Version 1.49u).
358 Values for body length were presented as mean body length in cm. All the experiments except
359 body length measurements (three times) were performed at least eight times.

360 **Phalloidin Staining**

361 Phalloidin staining was performed on 96 hpf embryos (N=8) as described[28]. Following fixation in
362 4% PFA and permeabilization with 50 µg/ml Proteinase K, embryos were incubated in Alexa-
363 Fluor 488 conjugated Phalloidin (Invitrogen, A12379) overnight at +4ºC. Embryos were then
364 mounted onto glass bottom dishes and photographed with Zeiss LSM Pascal laser scanning
365 confocal microscope. Somite lengths were measured by using ImageJ (Version 1.49u).

366 **Hematoxylin Eosin Staining**

367 Adult zebrafish were freshly frozen in methyl-butanol cooled down in liquid nitrogen and then
368 taken into O.C.T compound for sectioning. Tissue sections were incubated in hematoxylin for 5
369 minutes, 1% acid-alcohol solution for 1 minute, 1% ammoniac for 1 minute, eosin solution for 3
370 minutes respectively by washing with distilled water in between steps. Finally, sections were
371 washed with alcohol and xylene, and mounted. Sections were scanned with Nikon Eclipse E-400
372 microscope and photographed by DXM 1200F digital camera.

373 **Motility Assay**

374 For motility assay 48 hpf embryos from in-crosses of *desma*$^{kg97/+}$, *desmb*$^{kg156/+}$ or
375 *desma*$^{kg97/+}$;*desmb*$^{kg156/kg156}$ adults were used. Motility assays were performed by previously
376 described protocol[18]. A petri dish was placed on a transparent sheet with concentric circles 5 mm
377 apart. One embryo at a time was positioned in the centre of the dish and stimulated using a
378 dissection needle. The escape response of the embryo was recorded using a high-speed camera
379 (Huawei, Mate 10 Lite, 16 MP, 120 fps). The movements of the embryo—midpoint between the
380 two eyes—were tracked using a custom software that works based on template matching

381 algorithm. The elapsed time between the last frame before touch stimulus and the first frame after
382 the body of the fish contacts the 10 mm circle was computed from the digitized embryo movements
383 with a resolution of 8.3 ms (120 fps). Experiments were performed blindly and after video
384 accusation, DNA was extracted from each embryo for genotyping.

385 **Calcium Flux**

386 1-year-old fish were euthanized using overdose of tricaine (MS222, 300 mg/l). After removal of
387 the skin, tissue samples were incubated into 5 mg/ml collagenase solution in PBS (without Ca^{2+}
388 and Mg^{2+}) at 28.5 °C for 20 minutes on a shaker at 50 rpm. Samples have been triturated gently
389 under dissecting microscope in order to dissociate muscle fibres from the tissue components until
390 rode-shaped muscle fibres were obtained. Dissociated fibres were incubated in DMEM containing
391 10% FBS and 1% antibiotic-antimycotic overnight at 28.5 °C and 5% CO_2 environment. On the
392 following day, fibres were incubated in 2.5 μM Fluo-4 AM for 20 minutes in 5% CO_2. Under a
393 laser scanning confocal microscope (Zeiss LSM Pascal), glass microelectrodes (filled with 3M
394 KCl) were inserted into muscle fibres in a current clamp mode[29]. A depolarizing current stimulus
395 was delivered through the microelectrode to excite the fibre and evoke a calcium signal. The
396 evoked calcium-specific fluorescent emission signal was recorded in "Line Scan" mode of
397 confocal microscope, supplying information about a line cross sectioning the muscle fibre at a high
398 frequency in tandem with the electrical recordings. Data were analyzed in MATLAB (The
399 MathWorks, Inc). The stimulus waveform, which consisted of four consecutive pulses increasing
400 in duration, was used in all the experiments. The amplitude of the current pulse was kept constant
401 at 100 nA while the durations were 10 ms, 20 ms, 30 ms, 40 ms respectively. Experiments were
402 done by using three WT, three *desma*$^{kg97/kg97}$ and two *desmb*$^{kg156/kg156}$ fish and at least eight fibres
403 from each group were recorded.

404 ## Statistics

405 Data were statistically analyzed by GraphPad Prism 8 (GraphPad Software Inc.) by nonparametric
406 Mann-Whitney U test (Two-tailed) when two groups were compared. The results were considered
407 significant when $P<0.05$. For analysis of time course experiments (hatching rate, mortality rate
408 and time course calcium flux), repeated measures two-way ANOVA was used and Bonferroni post
409 *hoc* test was used for multiple comparisons. All error bars were presented as mean±SEM and bars
410 were represented as median.

Acknowledgements

This work was supported by The Scientific and Technological Research Council of Turkey, Project no. 214S174 to P.R.D. S.M.H. is an MRC Scientist with MRC Programme Grant G1001029 and MR/N021231/1 support.

Competing interests

The author(s) declare no competing interests.

Data Availability

Supporting information is available in Supplementary files online and further information is available from the corresponding author upon request.

References

1. Clemen, C. S., Herrmann, H., Strelkov, S. V. & Schröder, R. Desminopathies: Pathology and mechanisms. *Acta Neuropathologica* (2013) doi:10.1007/s00401-012-1057-6.
2. Dagvadorj, A. *et al.* Respiratory insufficiency in desminopathy patients caused by introduction of proline residues in desmin C-terminal α-helical segment. *Muscle and Nerve* (2003) doi:10.1002/mus.10370.
3. Ariza, A. *et al.* Desmin myopathy: a multisystem disorder involving skeletal, cardiac, and smooth muscle. *Hum. Pathol.* (1995) doi:10.1016/0046-8177(95)90095-0.
4. Goldfarb, L. G. *et al.* Missense mutations in desmin associated with familial cardiac and skeletal myopathy. *Nat. Genet.* (1998) doi:10.1038/1300.
5. Cetin, N. *et al.* A novel desmin mutation leading to autosomal recessive limb-girdle muscular dystrophy: distinct histopathological outcomes compared with desminopathies. *J. Med. Genet.* **50**, 437–43 (2013).
6. Bär, H. *et al.* Conspicuous involvement of desmin tail mutations in diverse cardiac and skeletal myopathies. *Hum. Mutat.* (2007) doi:10.1002/humu.20459.
7. Li, Z. *et al.* Cardiovascular lesions and skeletal myopathy in mice lacking desmin. *Dev. Biol.* (1996) doi:10.1006/dbio.1996.0122.
8. Milner, D. J., Weitzer, G., Tran, D., Bradley, A. & Capetanaki, Y. Disruption of muscle architecture and myocardial degeneration in mice lacking desmin. *J. Cell Biol.* (1996) doi:10.1083/jcb.134.5.1255.

440 9. Lin, Y. Y. Muscle diseases in the zebrafish. *Neuromuscular Disorders* (2012)
441 doi:10.1016/j.nmd.2012.04.007.
442 10. Berger, J. & Currie, P. D. Zebrafish models flex their muscles to shed light on muscular
443 dystrophies. *Dis. Model. Mech.* **5**, 726–32 (2012).
444 11. Gibbs, E. M., Horstick, E. J. & Dowling, J. J. Swimming into prominence: the zebrafish as
445 a valuable tool for studying human myopathies and muscular dystrophies. *FEBS J.* **280**,
446 4187–97 (2013).
447 12. Vogel, B. *et al.* In-vivo characterization of human dilated cardiomyopathy genes in
448 zebrafish. *Biochem. Biophys. Res. Commun.* **390**, 516–522 (2009).
449 13. Li, M., Andersson-Lendahl, M., Sejersen, T. & Arner, A. Knockdown of desmin in
450 zebrafish larvae affects interfilament spacing and mechanical properties of skeletal
451 muscle. *J. Gen. Physiol.* **141**, 335–345 (2013).
452 14. Ramspacher, C. *et al.* Developmental Alterations in Heart Biomechanics and Skeletal
453 Muscle Function in Desmin Mutants Suggest an Early Pathological Root for
454 Desminopathies. *Cell Rep.* **11**, 1564–76 (2015).
455 15. El-Brolosy, M. A. *et al.* Genetic compensation triggered by mutant mRNA degradation.
456 *Nature* **568**, 193–197 (2019).
457 16. Kimmel, C. B., Ballard, W. W., Kimmel, S. R., Ullmann, B. & Schilling, T. F. Stages of
458 Embryonic Development of the Zebrafish. *Dev. Dyn.* **203**, 253–310 (1995).
459 17. Skobo, T. *et al.* Zebrafish ambra1a and ambra1b knockdown impairs skeletal muscle
460 development. *PLoS One* (2014) doi:10.1371/journal.pone.0099210.
461 18. Goody, M. F. *et al.* NAD+ Biosynthesis Ameliorates a Zebrafish Model of Muscular
462 Dystrophy. *PLoS Biol.* (2012) doi:10.1371/journal.pbio.1001409.
463 19. Campbell, J. M., Hartjes, K. a, Nelson, T. J., Xu, X. & Ekker, S. C. New and TALENted
464 genome engineering toolbox. *Circ. Res.* **113**, 571–87 (2013).
465 20. Hnia, K., Ramspacher, C., Vermot, J. & Laporte, J. Desmin in muscle and associated
466 diseases: beyond the structural function. *Cell and Tissue Research* (2015)
467 doi:10.1007/s00441-014-2016-4.
468 21. Ramspacher, C. *et al.* Developmental Alterations in Heart Biomechanics and Skeletal
469 Muscle Function in Desmin Mutants Suggest an Early Pathological Root for
470 Desminopathies. *Cell Rep.* **11**, 1564–1576 (2015).

471 22. Kok, F. O. *et al.* Reverse genetic screening reveals poor correlation between morpholino-
472 induced and mutant phenotypes in zebrafish. *Dev. Cell* (2015)
473 doi:10.1016/j.devcel.2014.11.018.
474 23. Law, S. H. W. & Sargent, T. D. The serine-threonine protein kinase PAK4 is dispensable
475 in zebrafish: Identification of a morpholino-generated pseudophenotype. *PLoS One* (2014)
476 doi:10.1371/journal.pone.0100268.
477 24. Fin, L., Bergamin, G., Steiner, R. A. & Hughes, S. M. The Cannabinoid Receptor
478 Interacting Proteins 1 of zebrafish are not required for morphological development,
479 viability or fertility. *Sci. Rep.* **7**, 1–9 (2017).
480 25. Rossi, A. *et al.* Genetic compensation induced by deleterious mutations but not gene
481 knockdowns. *Nature* **524**, 230–233 (2015).
482 26. Hinits, Y. & Hughes, S. M. Mef2s are required for thick filament formation in nascent
483 muscle fibres. *Development* (2007) doi:10.1242/dev.007088.
484 27. Schmittgen, T. D. & Livak, K. J. Analyzing real-time PCR data by the comparative CT
485 method. *Nat. Protoc.* (2008) doi:10.1038/nprot.2008.73.
486 28. Goody, M. & Henry, C. http://www.bio-protocol.org/e786 Vol 3, Iss 11, Jun 05, 2013.
487 *Bio-Protocol* (2013).
488 29. Purali, N. Fast calcium transients translate the distribution and conduction of neural
489 activity in different regions of a single sensory neuron. *Invertebr. Neurosci.* (2017)
490 doi:10.1007/s10158-017-0201-3.

491 Author Contributions

492 P.R.D. designed, P.R.D. and S.M.H. supervised the study. G.K.K. wrote the paper, E.K.M. made
493 contribution to writing the paper and assembled the figures. G.K.K., E.K.M, C.K., S.U., B.S., B.E.,
494 I.U., N.D., B.T. and N.P. performed the experiments and/or analyzed the results. All authors
495 interpreted the data and edited the manuscript.

496 Figure Legends

497 **Fig. 1. Whole mount *in situ* mRNA hybridisation of embryos at the indicated stages for**
498 **antisense probes to *desma* and *desmb*.** (**a**) Lateral views are anterior to top, dorsal to left for 13-
499 22 hpf; anterior to left except 11 hpf which is a dorsal view. 48-120 hpf whole mounts are anterior

500 to left, dorsal to top. Scale bar: 250 µm. (**b**) Arrows indicate heart in frontal view for left panel
501 (*desma*) and ventral view for right panel (*desmb*) of 35 hpf embryos. (**c**) Transversal sections where
502 dorsal is top. (**d**) Upper left panel is a lateral view at 96 hpf, scale bar: 250 µm. Dashed line
503 represents the position of the transversal section in upper right panel where dorsal is top, scale bar:
504 100 µm. Lower panels are lateral views of zebrafish heads at 72 and 120 hpf treated with *desma*
505 probe. Scale bar: 100 µm. (**e**) Left panel is a ventral view with anterior at top. Right panels are
506 lateral views. Ai, anterior intestine; eom, extraocular muscles; fast, fast muscles; fm, pectoral fin
507 muscles; hm, hypaxial muscles; mdm, mandibular muscles; om, opercular muscles; slow, slow
508 muscles; som, somites. Scale bar: 250 µm.

509 **Fig. 2. Generation of *desma* and *desmb* knockout lines. (a**) Alignments and chromatograms of
510 wild-type DNA sequences with mutant alleles, and predicted mutant polypeptide sequences. In
511 DNA sequences, yellow highlights gRNA target sequence, hyphens show deleted bases, inserted
512 bases are indicated in red font. In protein sequences, the first residue affected by the frameshift is
513 indicated in red font, asterisks represent early stop codons. (**b**) Quantitative real-time PCR results
514 showing the expression of *desma* mRNA (upper graphic) and *desmb* mRNA (lower graphic) in
515 wild-type and homozygous mutant 96 hpf embryos (N=5). A significant decrease of *desma*
516 transcripts in $desma^{kg97}$ homozygous embryos (P=0.0119, Mann-Whitney U) was observed while
517 *desmb* transcripts were significantly decreased in $desmb^{kg156}$ homozygous embryos at 96 hpf
518 compared to WT (P=0.0079, Mann-Whitney U). (**c**) Left panel shows whole mount *in situ* mRNA
519 hybridisation of $desma^{kg97}$ homozygous embryos at the indicated stages for antisense probes to
520 *desmb*. Right panel shows whole mount *in situ* mRNA hybridisation of $desmb^{kg156}$ homozygous
521 embryos at the indicated stages for antisense probes to *desma.* Scale bar: 250 µm. Ai, anterior
522 intestine; som, somites. (**d-f**) Whole mount immunofluorescence staining of desmin with an anti-
523 desmin polyclonal antibody (Sigma, D8281) recognizing both Desma and Desmb, in wild-type
524 and mutant 96 hpf embryos. Scale bar: 500 µm. Boxes with dashed lines delineate areas that were
525 zoomed and focused on intestine. Pictures showing DAPI staining of each embryo are included at
526 their bottom right. (**d**) Upper panel is lateral view of a WT embryo with anterior to left, dorsal to
527 top. Lower panel is ventral view with anterior to left, arrowheads indicate the gut. (**e**) Upper panels
528 are lateral views of $desmb^{kg156/kg156}$ embryo with anterior to left, dorsal to top. Lower left panel

529 shows anterior intestine (orange arrowheads), lower right panel shows middle and posterior
530 intestine (white arrowheads). (**f**) Lateral view of *desma*$^{kg97/kg97}$ with anterior to left, dorsal to top.

531 **Fig. 3. Evaluation of neuromuscular defect in mutant larvae.** (**a)** The number of viable embryos
532 after successful mating of WT fish (n=10) compared to homozygous *desma*^{kg97} (n=10) (*P*=0.6842,
533 Mann-Whitney U) or homozygous *desmb*^{kg156} (n=8) (*P*=0.9654, Mann-Whitney U) fish. (**b)**
534 Comparison of hatching rate between homozygous mutants and WT 24, 48 and 72 hpf embryos
535 At 72 hpf, no significant difference in the hatching rate was found between mutants and WT
536 (*desma*$^{kg97/kg97}$ vs. WT, *P*=0.9902; *desmb*$^{kg156/kg156}$ vs WT, *P*=0.3186, repeated measures two-way
537 ANOVA, Bonferroni post *hoc* test) (**c)** Body length of 96 hpf WT (N=18) and homozygous
538 *desma*^{kg97} (N=25) or homozygous *desmb*^{kg156} (N=16) mutant embryos (*P*=0.2036 for WT vs.
539 *desma*$^{kg97/kg97}$; *P*=0.1893 for WT vs. *desmb*$^{kg156/kg156}$, Mann-Whitney U). (**d)** Cumulative mortality
540 rate from 1 to 5 dpf homozygous *desma*^{kg97} mutants (N=1247) compared to WT (N=2460)
541 (*P*=0.1287, repeated measures two-way ANOVA, Bonferroni post *hoc* test) and homozygous
542 *desmb*^{kg156} mutants (N=2615) compared to WT (*P*=0.6239, repeated measures two-way ANOVA,
543 Bonferroni post *hoc* test). **e.** Optical sections of the mid-trunk region of WT and homozygous
544 mutants 96 hpf embryos stained with phalloidin (N=8). Scale bars: 50 µm. (**f)** Somite lengths (µm,
545 N=8) were measured from optical sections of WT and mutant embryos stained with phalloidin
546 (*P*=0.7912 for WT vs. *desma*$^{kg97/kg97}$; *P*=0.4923 for WT vs. *desmb*$^{kg156/kg156}$, Mann-Whitney U). (**g-**
547 **i)** Touch-evoked escape time (ms) of 48 hpf embryos. Motility experiments were performed blind
548 on siblings from (**g**) *desma*$^{kg97/+}$, (**h**) *desmb*$^{kg156/+}$ or (**i**) *desma*$^{kg97/+}$*;desmb*$^{kg156/kg156}$ in-crosses
549 followed by *post hoc* genotyping. (**g**) Heterozygous *desma*^{kg97} embryos (N=23) were compared to
550 WT (N=9) (P=0.122, Mann-Whitney U) and *desma*$^{kg97/kg97}$ (N=15) compared to WT (P=0.5529,
551 Mann-Whitney U). (**h**) Heterozygous *desmb*^{kg156} embryos (N=6) were compared to WT (N=38)
552 (P=0.3968, Mann-Whitney U) and *desmb*$^{kg156/kg156}$ (N=6) compared to WT (P=0.6131, Mann-
553 Whitney U). (**i**) Homozygous double mutants (N=8) were compared to *desma*$^{+/+}$;*desmb*$^{kg156/kg156}$
554 (n=15) (*P*=0.3165, Mann-Whitney U) and *desma*$^{kg97/+}$*;desmb*$^{kg156/kg156}$ embryos (n=34) compared
555 to *desma*$^{+/+}$;*desmb*$^{kg156/kg156}$ (*P*=0.2334, Mann-Whitney U).

556 **Figure 4**. **Desmin protein expression and histological examination of adult skeletal muscle.**
557 **(a)** Immunoblotting of skeletal muscle protein extracts of WT, *desma*$^{kg97/kg97}$, *desma*$^{kg97/+}$,
558 *desmb*$^{kg156/kg156}$, *desmb*$^{kg156/+}$ and *desma*$^{kg97/kg97}$*;desmb*$^{kg156/kg156}$ double mutant fish, showing

559 expression of putative Desma-1 (55.7 kDa) and Desma-2 (54.1 kDa) isoforms. Lamin B1 was
560 labeled as loading control. (**b**) Transversal cryosections of mid-trunk somites from WT and
561 homozygous single and double mutant adults stained with hematoxylin eosin showing no
562 pathological changes. Scale bar: 250 µm.

563 **Fig. 5. Calcium flux in isolated fibres.** (**a**) Calcium flux along fibres was monitored in vivo by
564 Fluo-4 AM after four consecutive depolarizing stimuli. Top panel, membrane potential responses
565 to current stimulus pulses with varying durations of 10, 20, 30, 40 ms with the amplitude of the
566 current pulse kept constant at 100 mV and the duration increased by 10 ms at each pulse. Middle
567 panel, evoked calcium transients in line scan mode (*tx*) to current stimuli. Bottom panel, integrated
568 emission signal as a function of time for each experimental group. (**b**) Membrane potential
569 response to the first stimulus of 10 ms (top) or to the fourth stimulus of 40 ms. (**c**) Baseline
570 corrected amplitude divided by fibre diameter (ΔF/µm) of the calcium emission signals during the
571 first (10 ms) stimulus and fourth (40 ms) stimulus were compared between mutants and WT. (**e**)
572 Time course analysis of the baseline corrected and normalized amplitude of the calcium transient
573 from the longest stimulus (40 ms) was represented as mean amplitude values as a function of time.
574 Homozygous *desma*^{kg97} fibres (N=11, red curve) or homozygous *desmb*^{kg156} fibres (N=8, orange
575 curve) were compared to WT (N=8, blue curve). (* indicates time points where $P<0.05$, repeated
576 measures two-way ANOVA, Bonferroni post *hoc* test).

Figure 1.

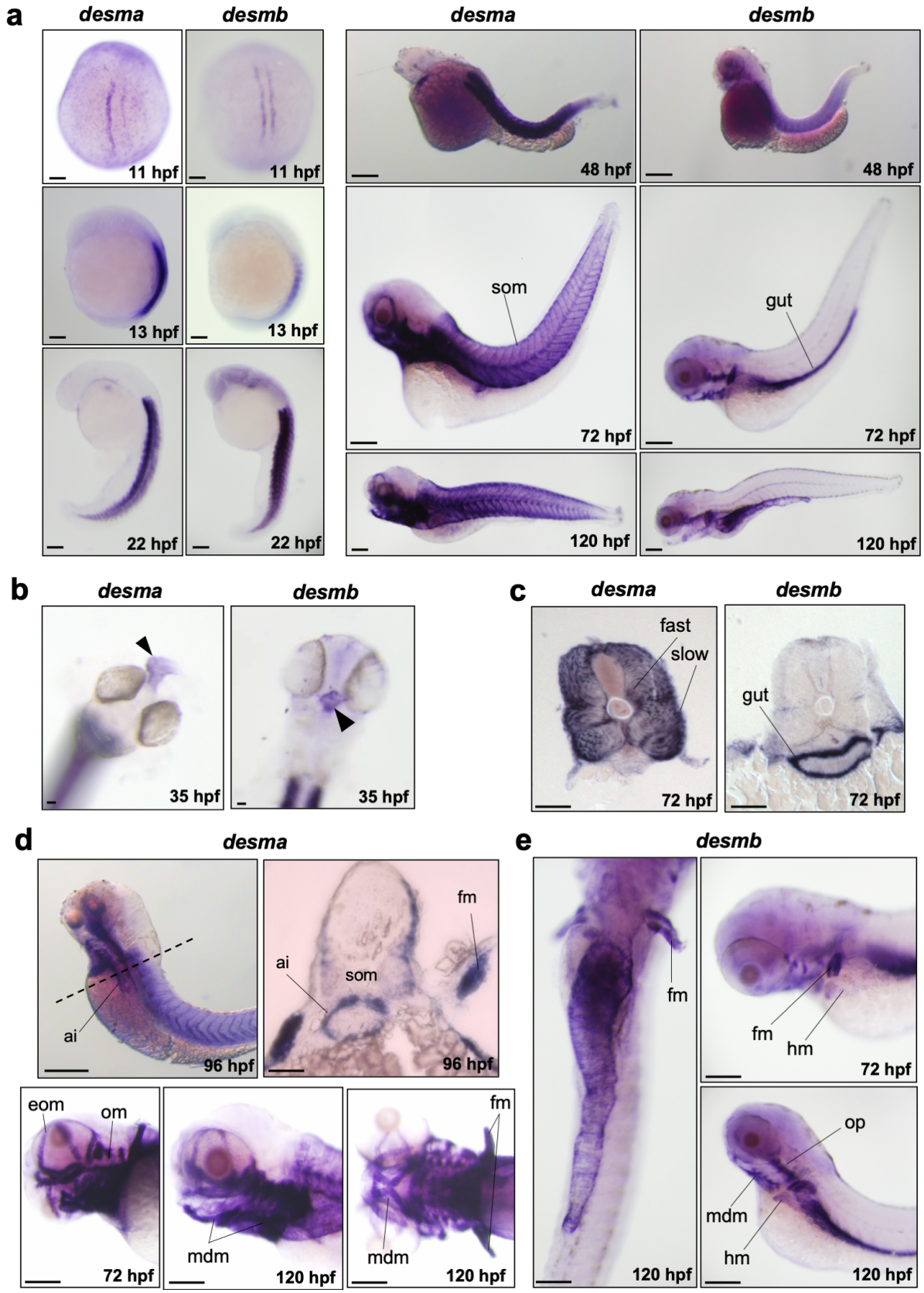
a
desma
desmb
desma
desmb
11 hpf
11 hpf
48 hpf
48 hpf
13 hpf
13 hpf
som
gut
22 hpf
22 hpf
72 hpf
72 hpf
120 hpf
120 hpf
b
desma
desmb
35 hpf
35 hpf
c
desma
desmb
fast
slow
gut
72 hpf
72 hpf
d
desma
ai
ai
som
fm
96 hpf
96 hpf
eom
om
mdm
mdm
fm
72 hpf
120 hpf
120 hpf
e
desmb
fm
fm
hm
op
mdm
hm
120 hpf
72 hpf
120 hpf

577

Figure 2.

a

desma

```
WT    CCTCAGGTTCCTCTGGCTCCTCAAGACTGACCTCCAGAGTTTACGAGGTGACCAAGAG
kg97  CCTCAGGTTCCTCTGGCTCCTCAAGACTGACCTCCA--TGATGTTTACGAGGTGACCA   -2+4
```

Protein sequence

```
WT    MSTKYSASAESASSYRRTFGSGLGSSIFAGHGSSGSSGSSRLTSRVYEVTKSSASPHF
kg97  MSTKYSASAESASSYRRTFGSGLGSSIFAGHGSSGSSGSSRLTSMMFTR*
```

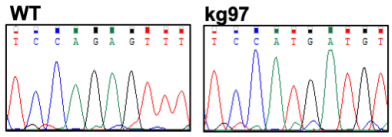

desmb

```
WT    CTCCTACAGCATGCCCAACTTGTCTGCAGGCTATACTCGCTCTTATGGTGGGATGGGT
kg156 CTCCTACAGCATGCCCAACTTGTCTGCAGGCTATACTCGCT-----GGTGGGATGGGT   -5
```

Protein sequence

```
WT    MSHSYATSSSSSYRRMFGGPGYMTP...PGFSGYRASSYSMPNLSAGYTRSYGGMGE
kg156 MSHSYATSSSSSYRRMFGGPGYMTP...PGFSGYRASSYSMPNLSAGYTRWWDG*
```

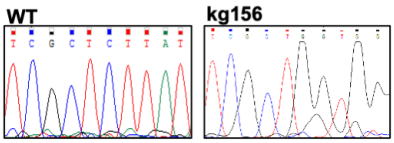

b

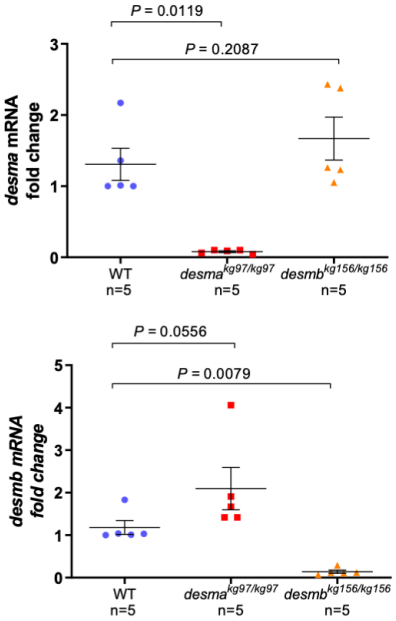

c

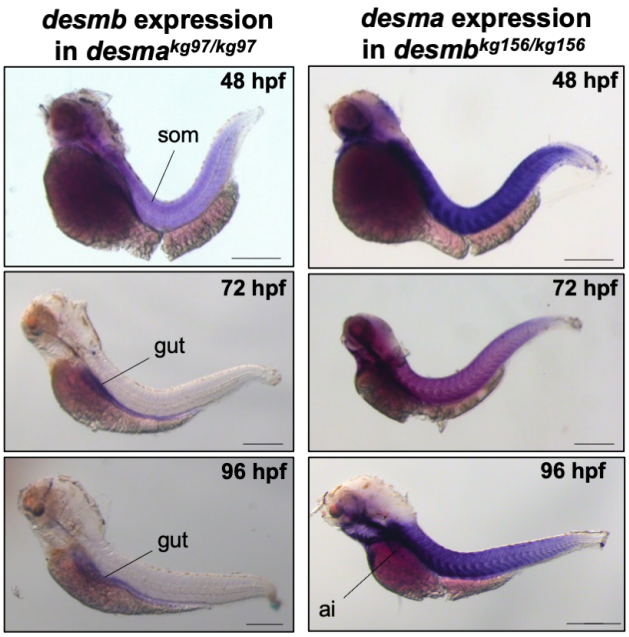

d

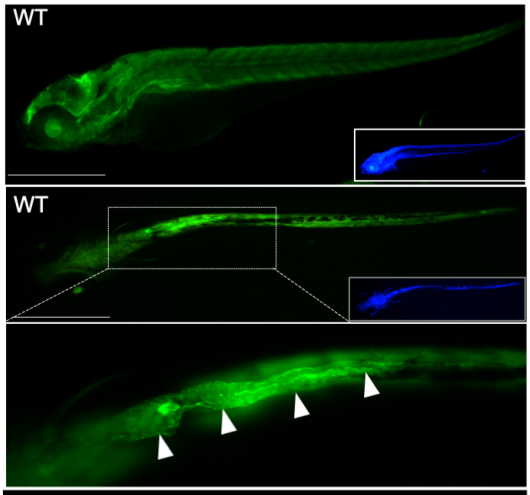

e

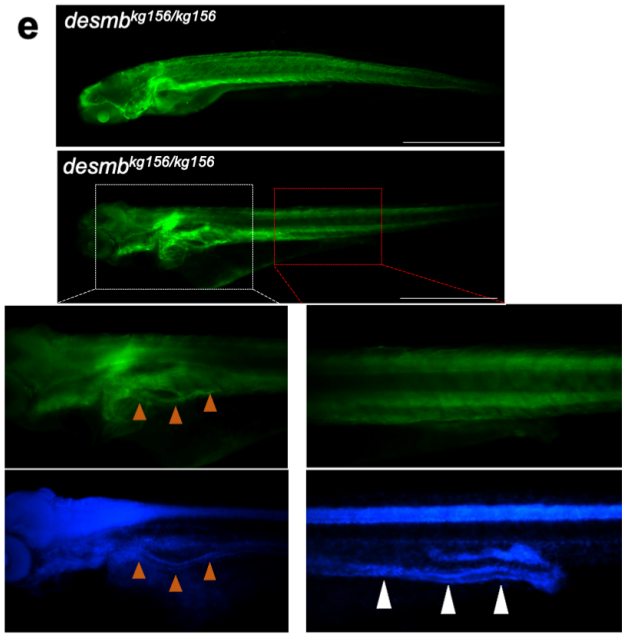

f

578

Figure 3.

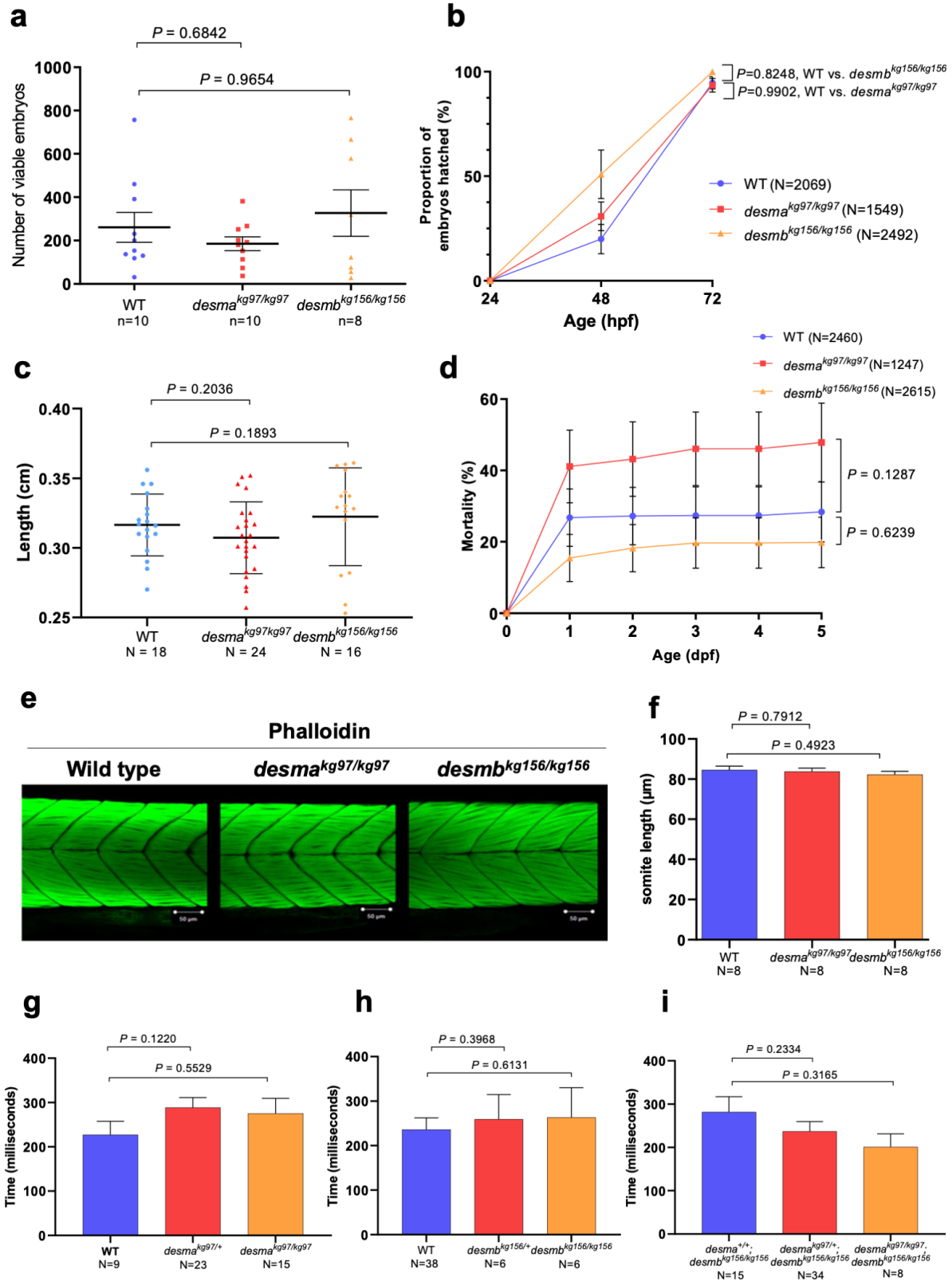
a
P = 0.6842
P = 0.9654
Number of viable embryos
1000
800
600
400
200
0
WT n=10
desma kg97/kg97 n=10
desmb kg156/kg156 n=8
b
P=0.8248, WT vs. desmb kg156/kg156
P=0.9902, WT vs. desma kg97/kg97
Proportion of embryos hatched (%)
100
50
0
24
48
72
Age (hpf)
WT (N=2069)
desma kg97/kg97 (N=1549)
desmb kg156/kg156 (N=2492)
c
P = 0.2036
P = 0.1893
Length (cm)
0.40
0.35
0.30
0.25
WT N = 18
desma kg97kg97 N = 24
desmb kg156/kg156 N = 16
d
WT (N=2460)
desma kg97/kg97 (N=1247)
desmb kg156/kg156 (N=2615)
Mortality (%)
60
40
20
0
P = 0.1287
P = 0.6239
0
1
2
3
4
5
Age (dpf)
e
Phalloidin
Wild type
desma kg97/kg97
desmb kg156/kg156
f
P = 0.7912
P = 0.4923
somite length (µm)
100
80
60
40
20
0
WT N=8
desma kg97/kg97 N=8
desmb kg156/kg156 N=8
g
P = 0.1220
P = 0.5529
Time (milliseconds)
400
300
200
100
0
WT N=9
desma kg97/+ N=23
desma kg97/kg97 N=15
h
P = 0.3968
P = 0.6131
Time (milliseconds)
400
300
200
100
0
WT N=38
desmb kg156/+ N=6
desmb kg156/kg156 N=6
i
P = 0.2334
P = 0.3165
Time (milliseconds)
400
300
200
100
0
desma +/+; desmb kg156/kg156 N=15
desma kg97/+; desmb kg156/kg156 N=34
desma kg97/kg97; desmb kg156/kg156 N=8

579

Figure 4.

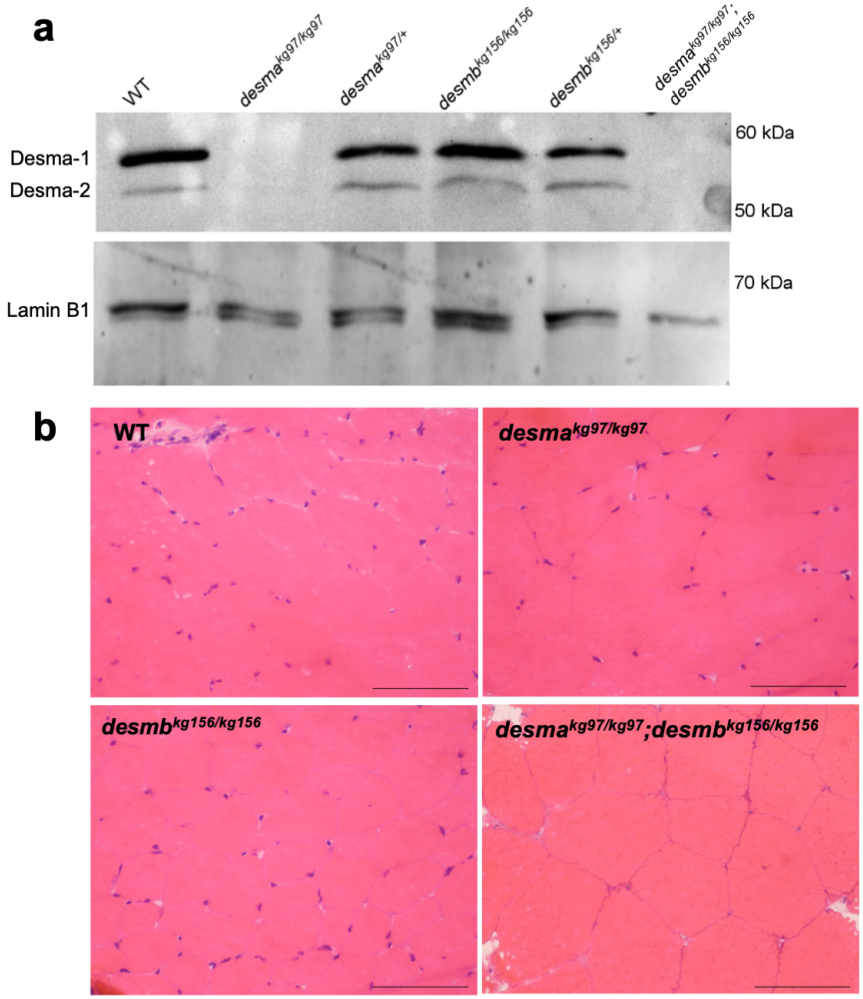
a
WT
desma kg97/kg97
desma kg97/+
desmb kg156/kg156
desmb kg156/+
desma kg97/kg97 ; desmb kg156/kg156
Desma-1
Desma-2
60 kDa
50 kDa
Lamin B1
70 kDa
b
WT
desma kg97/kg97
desmb kg156/kg156
desma kg97/kg97;desmb kg156/kg156

580

Figure 5.

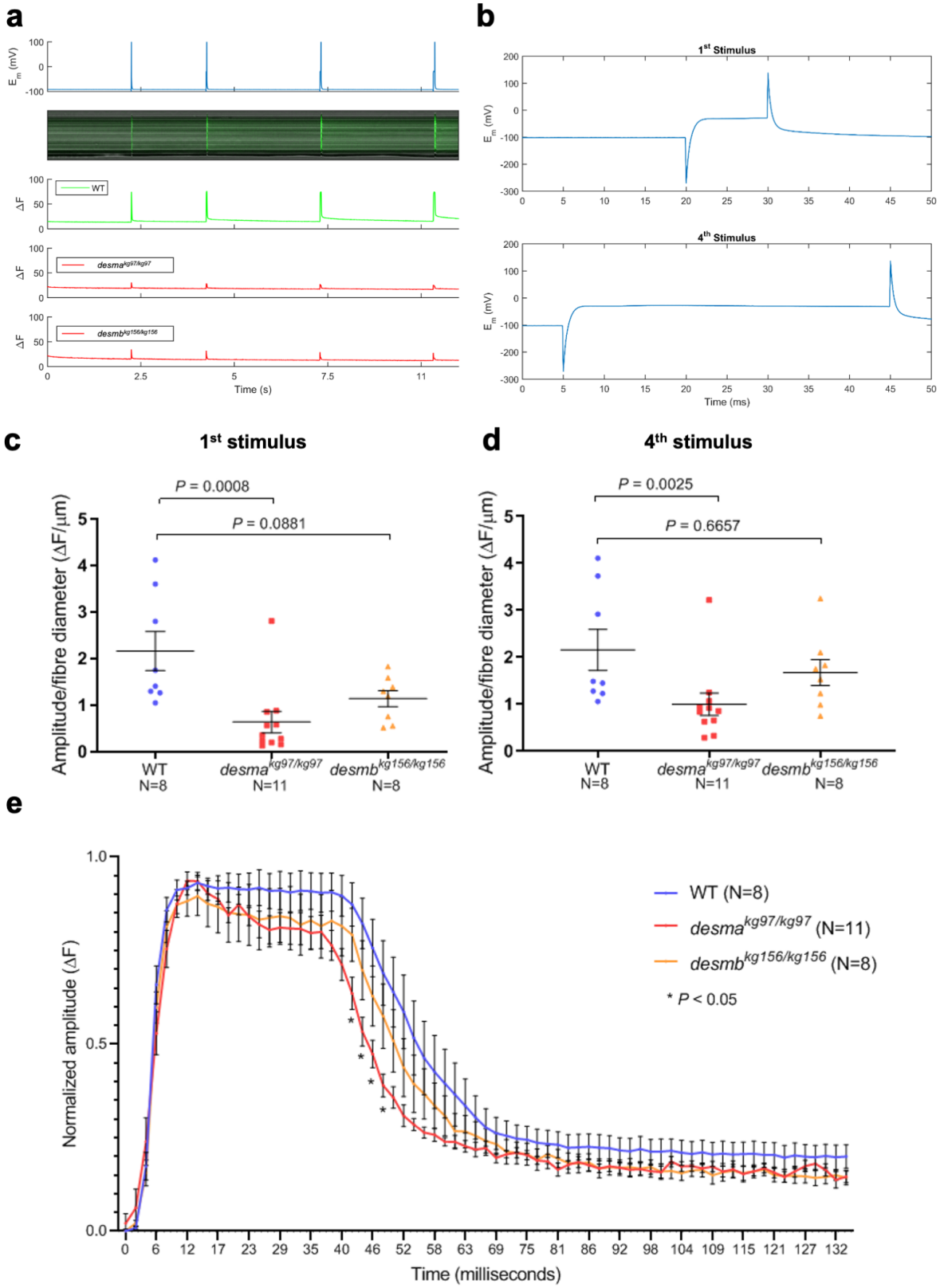
a
b
1st Stimulus
4th Stimulus
Time (s)
Time (ms)
c
1st stimulus
d
4th stimulus
P = 0.0008
P = 0.0881
P = 0.0025
P = 0.6657
Amplitude/fibre diameter (ΔF/μm)
WT N=8
desmakg97/kg97 N=11
desmbkg156/kg156 N=8
e
Normalized amplitude (ΔF)
Time (milliseconds)
WT (N=8)
desmakg97/kg97 (N=11)
desmbkg156/kg156 (N=8)
* P < 0.05

581